

## **REAL-TIME ESTIMATION OF IONOSPHERIC DELAY USING DUAL FREQUENCY GPS OBSERVATIONS**

*Dhiraj Sunehra, M.Tech., PhD*

Jawaharlal Nehru Technological University Hyderabad, Andhra Pradesh, India

---

### **Abstract**

The Global Navigation Satellite System (GNSS) is a space-based radio positioning system that includes one or more satellite constellations capable of providing three-dimensional position, velocity and time information continuously to users anywhere on, or near, the surface of the earth. The Global Positioning System (GPS) is the most well known GNSS and is operated by the U.S. Department of Defense. A GPS receiver uses two types of measurements, viz. code and carrier phase for determining its (user) position. The positional accuracy of GNSS is limited by several sources of error such as satellite and receiver clock offsets, signal propagation delays due to ionosphere and troposphere, multipath, receiver measurement noise and instrumental biases. The ionospheric delay is the most predominant of all the error sources. This delay is a function of the total electron content (TEC). Because of the dispersive nature of the ionosphere, one can estimate the ionospheric delay using the dual frequency GPS measurements. In this paper, two prominent ionospheric delay smoothing algorithms, viz. combined code and carrier smoothing filter (CCCSF) and Hatch smoothing filter (HSF) are compared for reducing the effect of code measurement noise and multipath. The smoothing results are validated with the Bernese GPS data processing software. The estimated TEC results after correction of various errors and biases are presented for various GAGAN stations. The work presented is useful for accurate ionospheric modeling required for communication, navigation and surveillance (CNS) systems in India.

---

**Keywords:** GPS, GAGAN, Ionospheric delay, TEC, Smoothing algorithms

### **Introduction**

There are three prominent Global Navigation Satellite System (GNSS) constellations around the world. The Global Positioning System (GPS) is the most well known and achieved full operational capability (FOC) in July 1995 with 24 Block II/IIA satellites. A

second configuration called the Global Orbiting Navigation Satellite System (GLONASS) is maintained by the Russian Republic. GLONASS system consists of 24 operational satellites and has regained its FOC in December 2011 (Website 1). The Galileo system is the third satellite based navigation system and is currently under development. Over the past decade, the number of civilian applications of GPS has increased significantly, as it provides reasonably good positioning accuracy in a cost effective manner. With the availability of multiple satellite constellations in the near future, the GNSS receiver would be capable of providing position information even in partially shadowed regions such as urban areas, forests, etc. The positional accuracy of GNSS is affected by several errors such as satellite and receiver clock errors, signal propagation delay errors due to ionosphere and troposphere, multipath error, receiver measurement noise and instrumental biases. Among all the error sources, ionospheric delay is the most predominant one and is of the order of 5-15m during mid-afternoon (El-Rabbany, 2002). The current level of accuracy, integrity and availability provided by the standalone GPS does not meet the more stringent air navigation requirements, particularly during the critical phases of flight like non-precision and precision approaches. For using GPS in precise positioning and navigation, satellite based augmentation systems (SBAS) have been planned by various countries including USA, Europe, Japan and India. The Indian SBAS known as GPS Aided Geo Augmented Navigation (GAGAN) is being jointly implemented by the Airports Authority of India (AAI) and Indian Space Research Organisation (ISRO) to provide seamless coverage over the Indian airspace and meet the navigation accuracy requirements of Category-I precision approach (CAT-I PA) and landing of aircrafts. (Suryanarayana Rao, 2007). As part of the GAGAN programme, several dual frequency GPS receivers are located at various airports around the Indian subcontinent. In order to meet the CAT-I PA requirements, accurate estimation of ionospheric delay is necessary. One can use either the dual frequency code or carrier phase measurements for estimating the ionospheric delay. The ionospheric delay obtained from the code measurements is unambiguous, but coarse in nature. On the other hand, that obtained from the carrier phase measurements is precise, but ambiguous. The measurement error (rms) due to receiver noise and multipath in code is about 0.5 - 1.0 m and that due to carrier phase measurement is of the order of 0.5 - 1 cm (Misra and Enge, 2001). The algorithms presented in this paper make use of the relative merits of both code and carrier phase measurements for reducing the effect of receiver measurement noise and multipath. Also, the instrumental delays (biases) of the satellite and receiver affect the ionospheric delay measurements obtained from a dual frequency receiver. The instrumental

delay due to the satellite can cause an error as large as 1.5 m in the ionospheric delay estimate, whereas the instrumental delay due to the receiver can be as large as 5 m. In order to estimate the ionospheric delay accurately, these instrumental biases are to be estimated.

### Prominent Ionospheric Delay Smoothing Algorithms

In this section, three prominent ionospheric delay smoothing algorithms are briefly discussed. The first algorithm named as combined code and carrier smoothing filter (CCCSF) uses the variances of the code and carrier phase data to minimize the receiver measurement noise and multipath, where as the second algorithm is an averaging technique based on the Hatch filter. The third algorithm is provided within the Bernese software, which is used for validation purpose. The first two techniques are recursive in nature, whereas the third technique is non-recursive.

#### Combined Code And Carrier Smoothing

The combined code and carrier smoothing filter (CCCSF) is a recursive technique for minimizing the effect of receiver measurement noise and multipath. The ionospheric delay ( $\tilde{I}_k$ ) at time  $t_k$  is estimated from the code and carrier phase measurements of the current epoch, the previous estimate ( $\tilde{I}_{k-1}$ ), and two weighting functions ( $w_1$  and  $w_2$ ) that are derived from the variances of the code and carrier measurements. The smoothed ionospheric delay at time  $t_k$  is computed as follows (Gao et al, 2002),

$$\tilde{I}_k = -\frac{(w_1)_k}{(w_1)_k + (w_2)_k} (P_1 - P_2)_k + \frac{(w_2)_k}{(w_1)_k + (w_2)_k} [\tilde{I}_{k-1} + \delta(\phi_1 - \phi_2)_k] \quad (1)$$

$$\text{where } (w_1)_k = \frac{1}{\sigma^2_{(P_1-P_2)_k}} \quad (2)$$

$$(w_2)_k = \frac{1}{\sigma^2_{(P_1-P_2)_k} + \sigma^2_{\delta(\phi_1-\phi_2)_k}} \quad (3)$$

$$\text{and } \delta(\phi_1 - \phi_2)_k = (\phi_1 - \phi_2)_k - (\phi_1 - \phi_2)_{k-1} \quad (4)$$

$P_1, P_2$  are the code measurements,  $\phi_1, \phi_2$  are the corresponding carrier phase measurements and  $\delta(\phi_1 - \phi_2)_k$  represents the change in the carrier ionospheric delay at time  $t_k$  from  $t_{k-1}$ .

#### Hatch Smoothing Filter

The Hatch smoothing filter (HSF) developed by Mr. Ron Hatch during eighties is based on the concept that the change in code range between observations at different time epochs equals the change in carrier range (Hatch, 1982). Using this condition, 'N' equations (for 'N' observations) can be formulated for the code ionospheric delay,  $(P_2 - P_1)_N$  at  $N^{\text{th}}$  epoch. The expression for the smoothed ionospheric delay is obtained by taking the average

of these ‘N’ equations. The Hatch filter for estimation of smoothed ionospheric delay can be represented in recursive form as,

$$(P_2 - P_1)'_N = (P_2 - P_1)_N / N + \{(P_2 - P_1)'_{N-1} + (\phi_1 - \phi_2)_N - (\phi_1 - \phi_2)_{N-1}\} \times (N-1) / N \quad (5)$$

where  $(P_2 - P_1)'_N$  is the smoothed differential ionospheric delay at N<sup>th</sup> epoch.  $(P_2 - P_1)'_{N-1}$  is the smoothed differential ionospheric delay at (N-1)th epoch.  $(P_2 - P_1)_N$  is the code differential ionospheric delay at N<sup>th</sup> epoch.  $(\phi_1 - \phi_2)_N$  is the carrier differential ionospheric delay at N<sup>th</sup> epoch. The precision of the smoothed ionospheric delay estimate is a direct function of the number of epochs N.

### Bernese Smoothing Algorithm

The Bernese GPS Software is developed at the Astronomical Institute University of Berne (AIUB), Switzerland and is widely used around the world. The Bernese GPS software (version 4.2) provides many algorithms for processing GPS data including one for smoothing (Hugentobler et al, 2001). The smoothed code on L1 ( $f_1$ ) frequency is given by,

$$P'_{1N} = \phi_{1N} + \bar{P}_1 - \bar{\phi}_1 + 2 \times \left( \frac{f_2^2}{f_1^2 - f_2^2} \right) \times ((\phi_{1N} - \phi_{2N}) - (\bar{\phi}_1 - \bar{\phi}_2)) \quad (6)$$

The smoothed code on L2 ( $f_2$ ) frequency is given by,

$$P'_{2N} = \phi_{2N} + \bar{P}_2 - \bar{\phi}_2 + 2 \times \left( \frac{f_1^2}{f_1^2 - f_2^2} \right) \times ((\phi_{1N} - \phi_{2N}) - (\bar{\phi}_1 - \bar{\phi}_2)) \quad (7)$$

where  $P'_{kN}$  is the smoothed code measurement at epoch N (on frequency  $f_k$ ,  $k=1, 2$ ).  $\phi_{kN}$  is the carrier phase measurement at epoch N (on frequency  $f_k$ ).  $\bar{P}_k - \bar{\phi}_k$  is the mean difference between all the code and phase measurements (on frequency  $f_k$ ).  $\bar{\phi}_1 - \bar{\phi}_2$  is the mean ionospheric delay over all the phase measurements.

By subtracting equation (7) from (6), the differential ionospheric delay is obtained.

### Comparative Results of Ionospheric Delay Smoothing Algorithms

In this investigation, dual frequency GPS data in Receiver Independent Exchange (RINEX) observation format is considered. The data corresponds to the Hyderabad GAGAN station (4<sup>th</sup> March 2005) and is provided by the Space Applications Centre (SAC), ISRO, Ahmedabad. The sampling rate of the data is 60s. The raw code ionospheric delay and the corresponding carrier phase ionospheric delay for PRN 30 are shown in Fig. 1. It can be observed that the code ionospheric delay is more noisy than the carrier ionospheric delay. However, carrier phase provides only relative delay due to integer ambiguity problem. The

smoothed ionospheric delay (PRN 30) obtained due to CCCSF and HSF are compared with corresponding Bernese software output in Fig. 2.

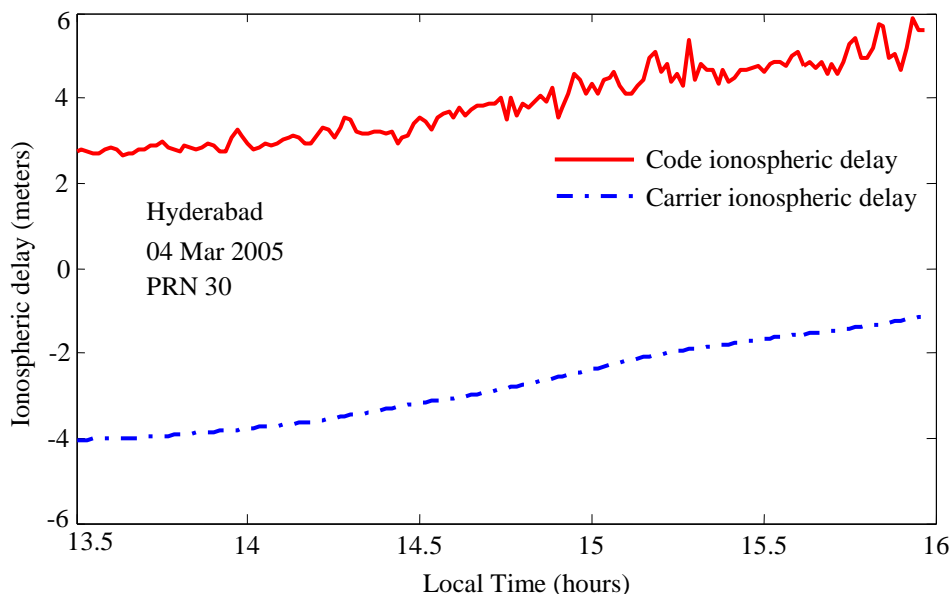


**Fig. 1** Ionospheric delay using code and carrier measurements

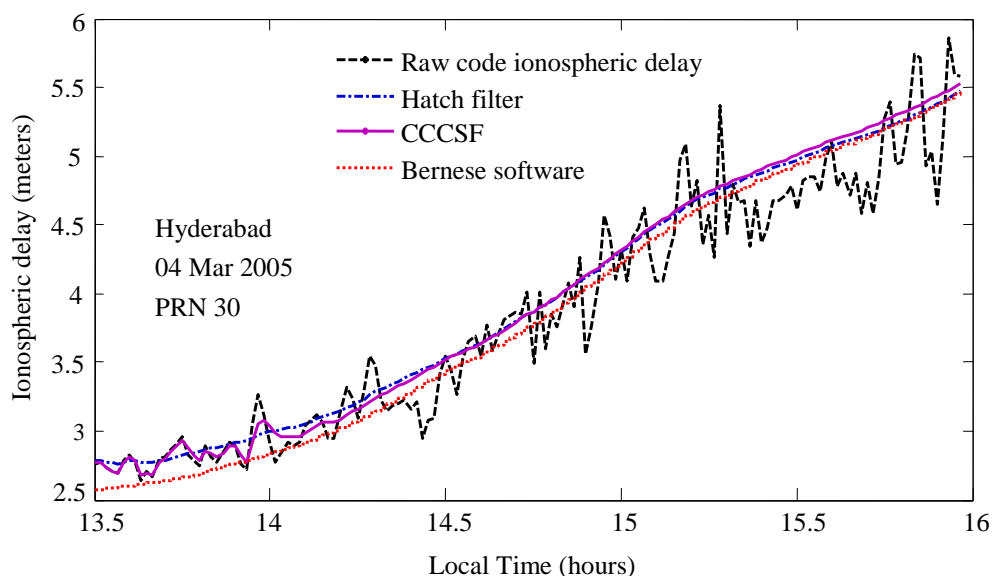


**Fig. 2** Comparison of ionospheric delay due to raw code, Hatch, CCCSF and Bernese

It can be observed from Fig. 2 that there is significant reduction in the noise after smoothing. It is found that the CCCSF algorithm is taking comparatively more time for convergence. The smoothing results due to both the algorithms closely follow Bernese output, with Hatch filter performing slightly better for most of the observation period. To evaluate the performance of these two algorithms, the difference between the smoothed version and unsmoothed version at each instant are calculated. For these differences mean, standard deviation ( $\sigma$ ), and RMS values due to the CCCSF, Hatch filter and Bernese are

statistically compared in Table 1 for four satellites (PRN 30, 2, 6 and 29) visible during the observation period.

**Table 1** Parameters describing the difference between smoothed and unsmoothed version

| Hatch Smoothing Filter (HSF) |          |              |         | Combined Code and Carrier Smoothing Filter (CCCSF) |              |         | Bernese software |              |         |
|------------------------------|----------|--------------|---------|--|--------------|---------|------------------|--------------|---------|
| PRN                          | Mean (m) | $\sigma$ (m) | RMS (m) | Mean (m)   | $\sigma$ (m) | RMS (m) | Mean (m)         | $\sigma$ (m) | RMS (m) |
| 30                           | -0.093   | 0.23         | 0.239   | -0.095   | 0.227        | 0.245   | -0.016           | 0.241        | 0.24    |
| 2                            | -0.098   | 0.307        | 0.319   | -0.116   | 0.308        | 0.326   | -0.098           | 0.307        | 0.319   |
| 6                            | -0.095   | 0.131        | 0.161   | -0.101   | 0.143        | 0.175   | 0.186            | 0.164        | 0.24    |
| 29                           | -0.021   | 0.143        | 0.144   | -0.002   | 0.136        | 0.135   | 0.039            | 0.147        | 0.152   |

For PRN 30, PRN 2 and PRN 29, standard deviation ( $\sigma$ ) and RMS values obtained from HSF algorithm are closer to the corresponding values obtained from Bernese software, whereas for PRN 6, CCCSF algorithm values are closer to the Bernese results.

#### TEC Results due to various GAGAN stations

The TEC over a day is estimated for various GAGAN stations considering Hatch Smoothing Filter (HSF).

(i) **Guwahati GAGAN station:** The slant TEC obtained using the code measurements of various satellites is shown in Fig. 3. The corresponding slant TEC computed from carrier phase measurements are shown in Fig. 4. The phase smoothed slant TEC obtained using HSF is shown in Fig. 5.

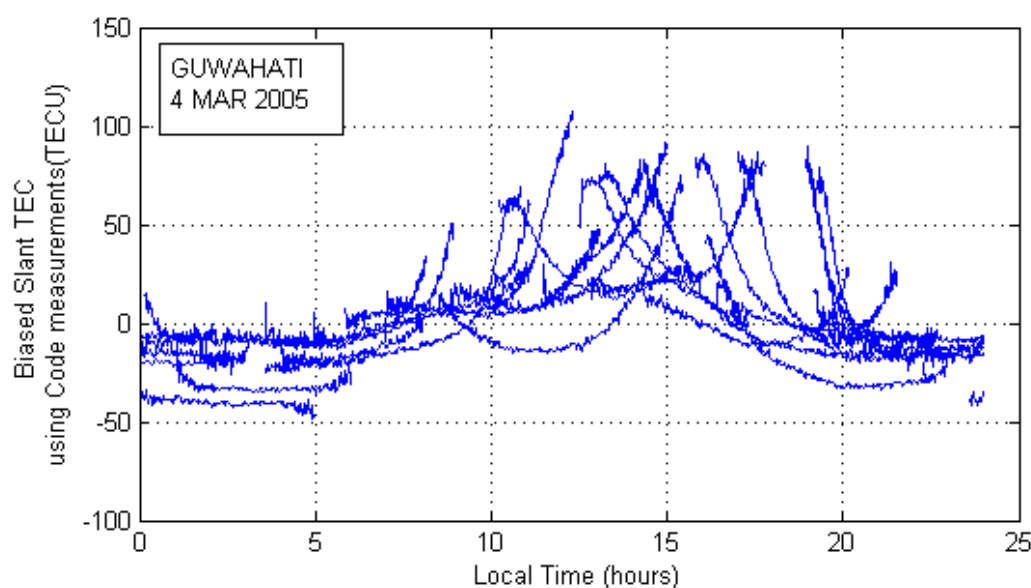


**Fig. 3** Slant TEC computed from code measurements (Guwahati)

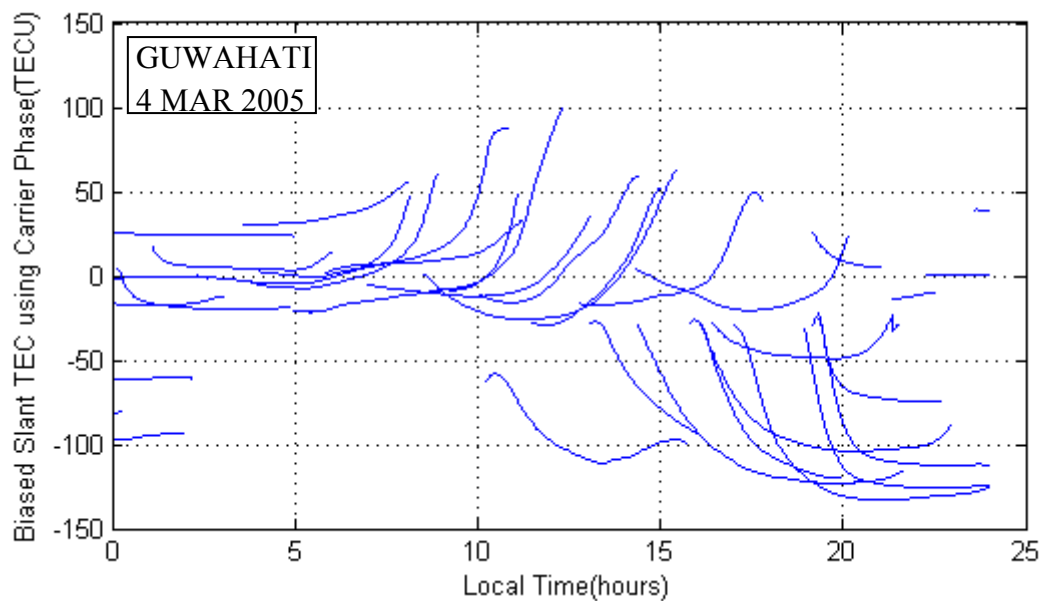


**Fig. 4** Slant TEC computed from carrier phase measurements (Guwahati)

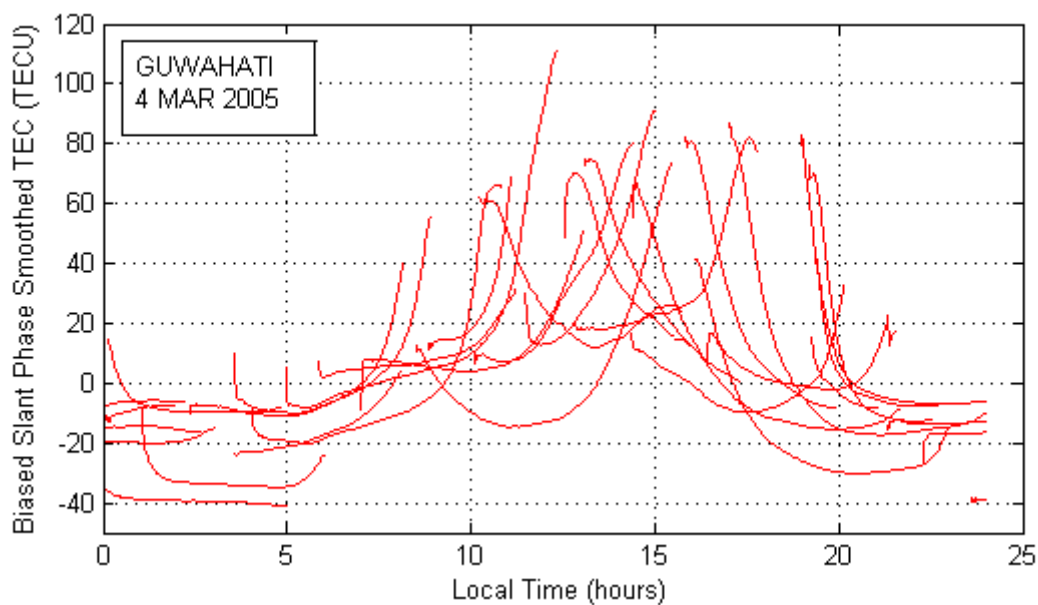


**Fig. 5** Phase smoothed slant TEC using Hatch smoothing filter (Guwahati)

The corresponding estimated vertical TEC after removing the instrumental bias error is shown in Fig. 6. The procedure for estimation of instrumental bias error using a Kalman filter is reported in Sunehra et al (2010).

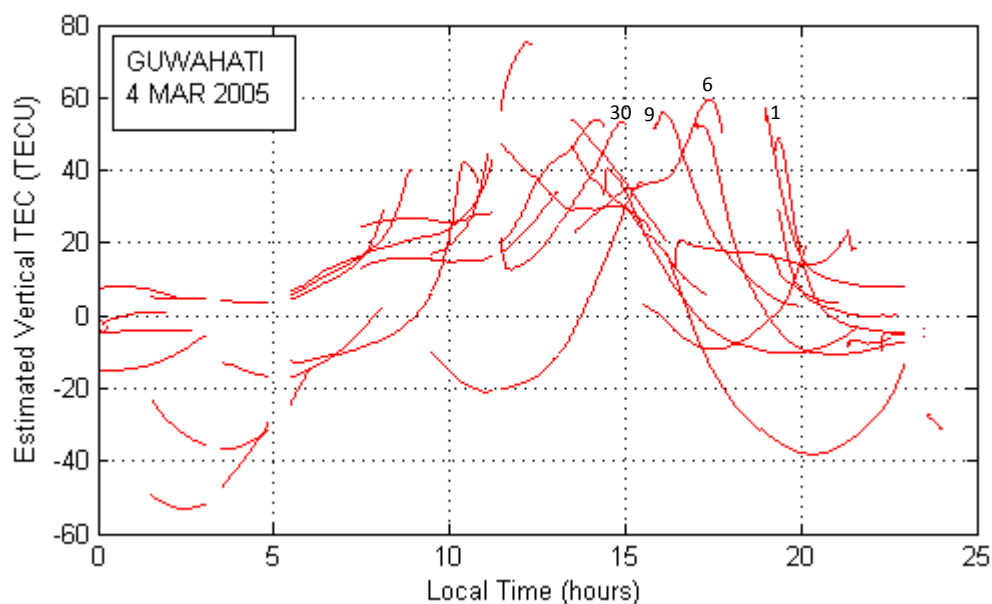


**Fig. 6** Estimated vertical TEC after correcting for instrumental biases (Guwahati)

The estimated maximum vertical TEC of two satellites, viz. PRN 6 and PRN 9 visible during mid-day, after correcting for instrumental biases are 59.0 and 56.0 TECU. The estimated mean value of receiver bias due to various satellites using Kalman filter is -1.8 ns.

**(ii) Mumbai GAGAN station:** The slant TEC obtained using the code measurements of various satellites is shown in Fig.7. The corresponding slant TEC computed from carrier phase measurements are shown in Fig. 8. The phase smoothed slant TEC obtained using HSF is shown in Fig. 9.

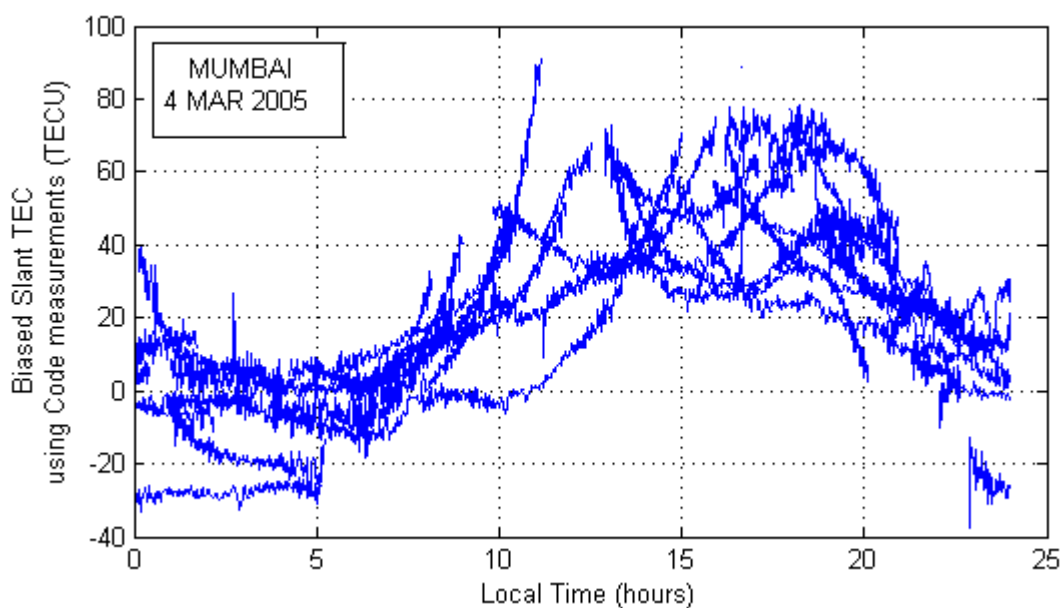


**Fig. 7** Slant TEC computed from code measurements (Mumbai)



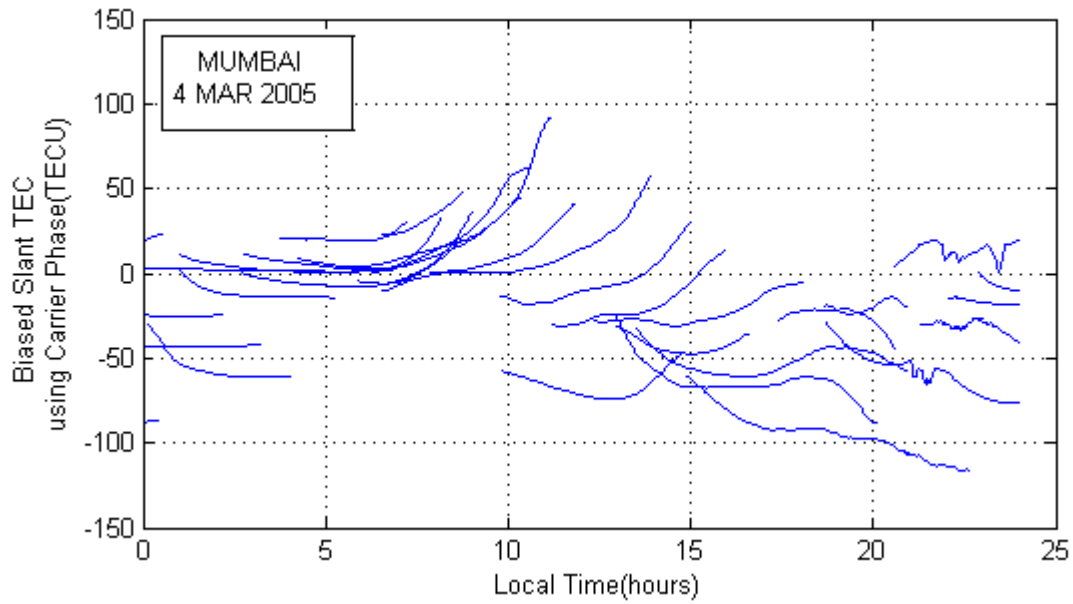


**Fig. 8** Slant TEC computed from carrier phase measurements (Mumbai)

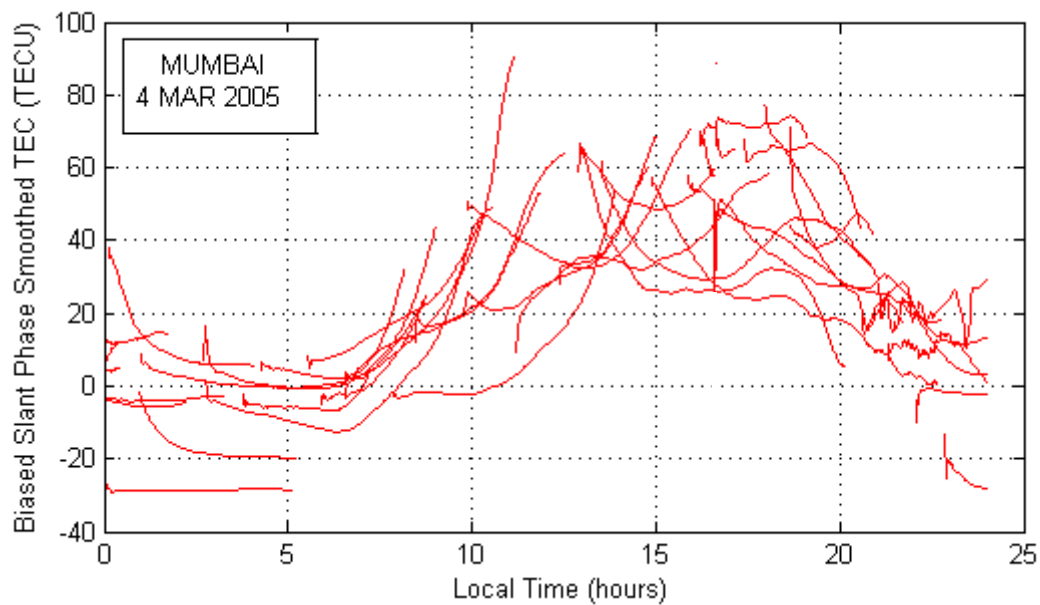


**Fig. 9** Phase smoothed slant TEC using Hatch smoothing filter (Mumbai)

The corresponding estimated vertical TEC after removing the instrumental bias error is shown in Fig. 10.

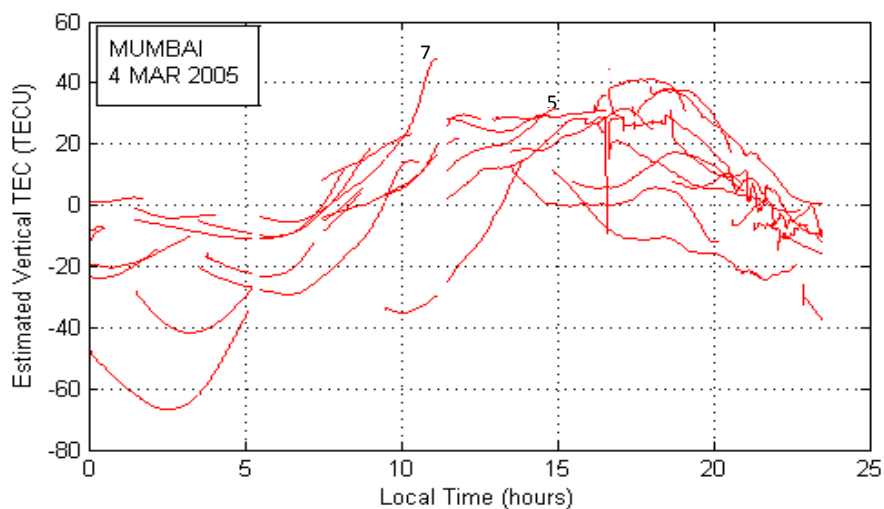


**Fig. 10** Estimated vertical TEC after correcting for instrumental biases (Mumbai)

The estimated maximum vertical TEC of two satellites, viz. PRN 7 and PRN 5 visible during mid-day, after correcting for instrumental biases are 47.8 and 31.6 TECU. The estimated mean value of receiver bias due to various satellites using Kalman filter is 5.2 ns.

**(iii) Lucknow GAGAN station:** The slant TEC obtained using the code measurements of various satellites is shown in Fig. 11. The corresponding slant TEC computed from carrier phase measurements are shown in Fig. 12. The phase smoothed slant TEC using the HSF is shown in Fig. 13.

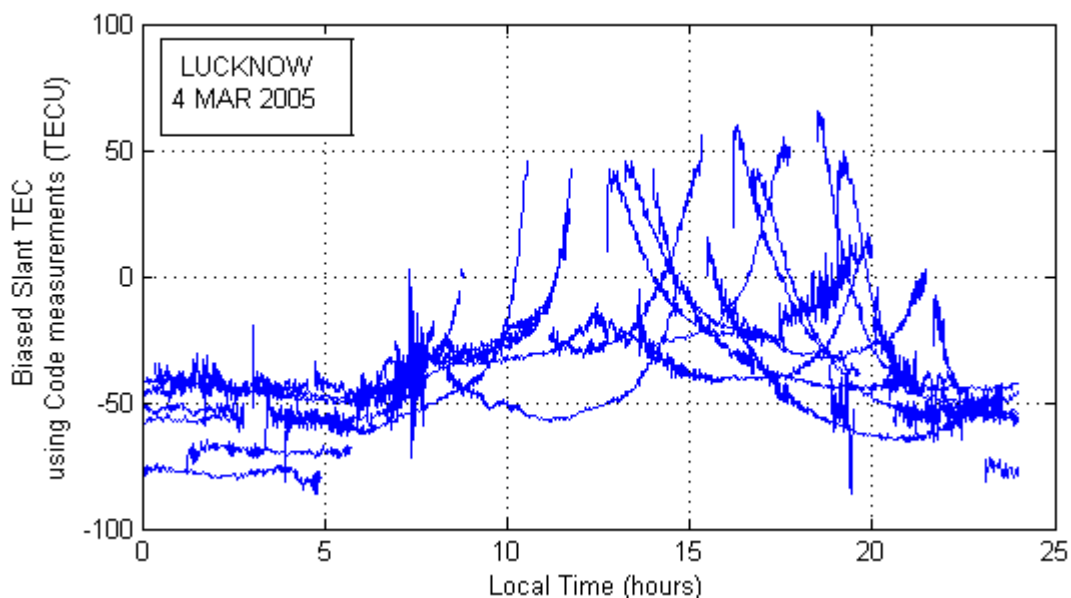


**Fig. 11** Slant TEC computed from code measurements (Lucknow)

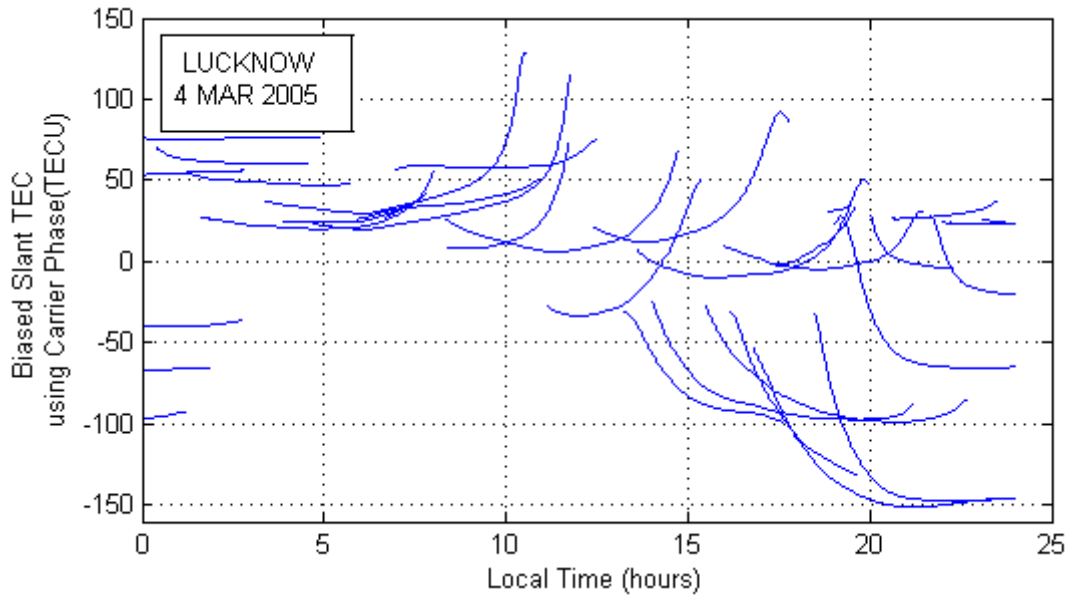


**Fig. 12** Slant TEC computed from carrier phase measurements (Lucknow)

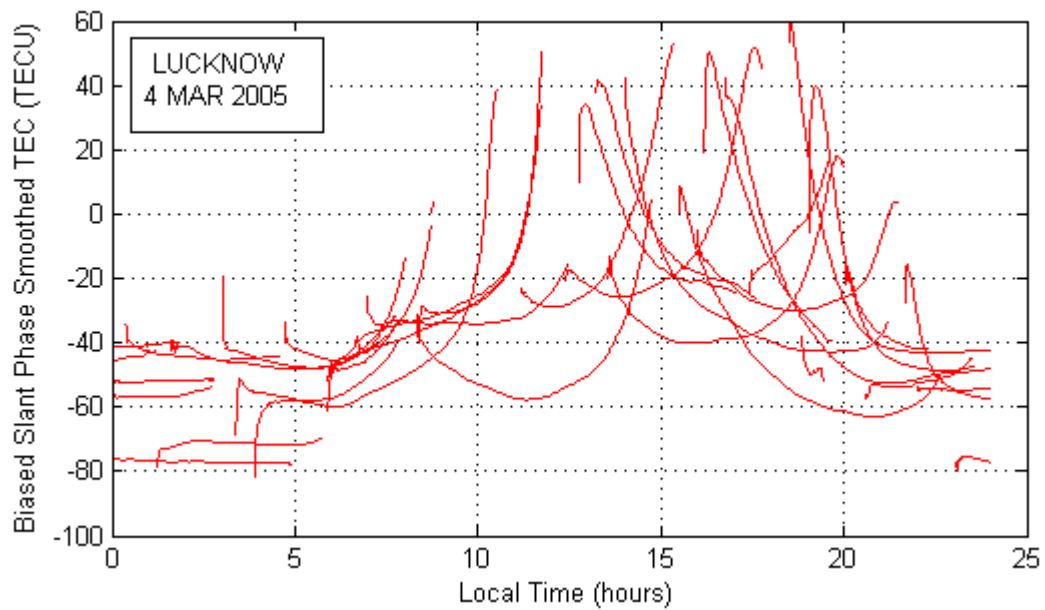


**Fig. 13** Phase smoothed slant TEC using Hatch smoothing filter (Lucknow)

The corresponding estimated vertical TEC after removing the instrumental bias error is shown in Fig. 14.

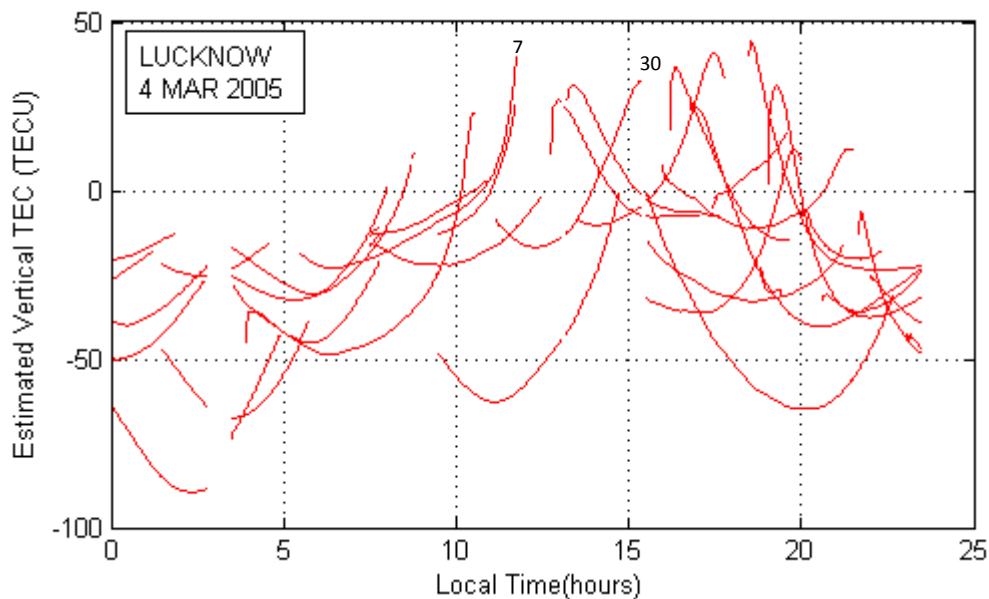


**Fig. 14** Estimated vertical TEC after correcting for instrumental biases (Lucknow)

The estimated maximum vertical TEC of two satellites, viz. PRN 7 and PRN 30 visible during mid-day, after correcting for instrumental biases are 39.3 and 32.4 TECU. The estimated mean value of receiver bias due to various satellites using Kalman filter is -1.6 ns.

*(iv) Thiruvananthapuram GAGAN station:* The slant TEC obtained using the code measurements of various satellites is shown in Fig. 15. The corresponding slant TEC computed from carrier phase measurements are shown in Fig. 16. The phase smoothed slant TEC using the HSF is shown in Fig. 17.

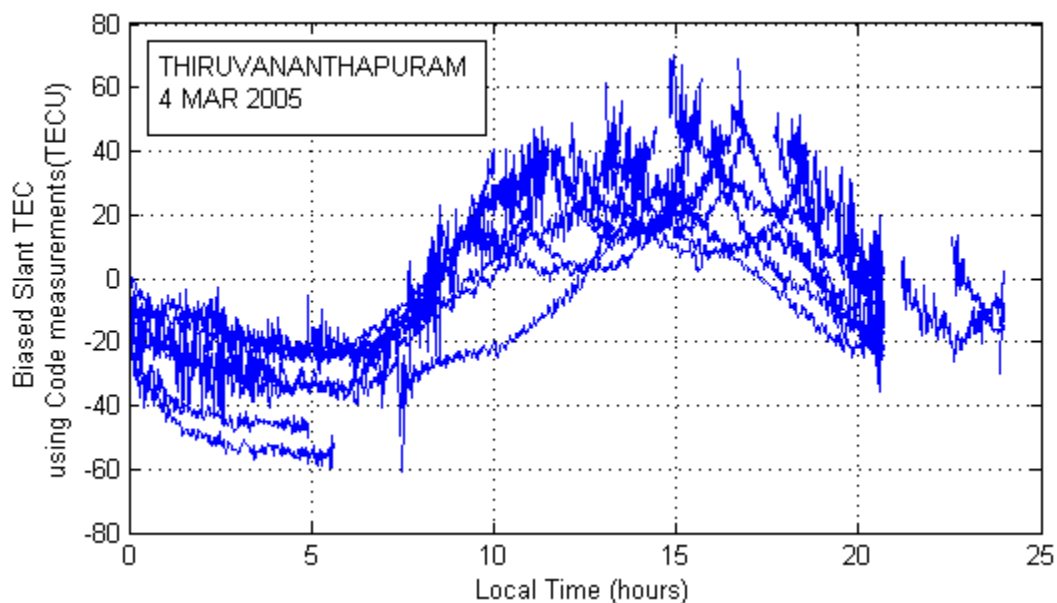


**Fig. 15** Slant TEC computed from code measurements (Thiruvananthapuram)

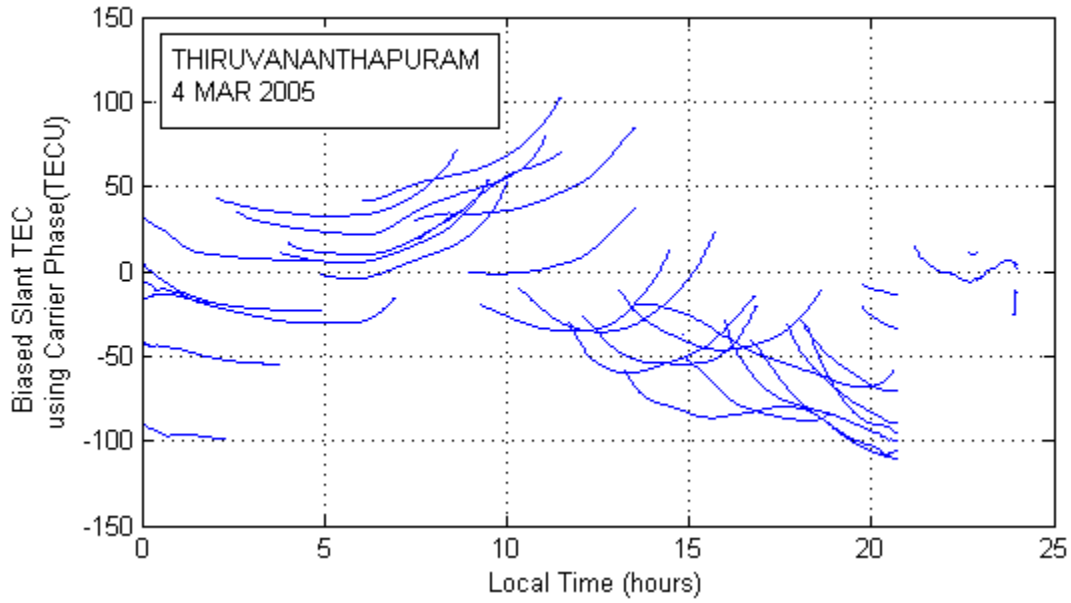


**Fig. 16** Slant TEC computed from carrier phase measurements (Thiruvananthapuram)

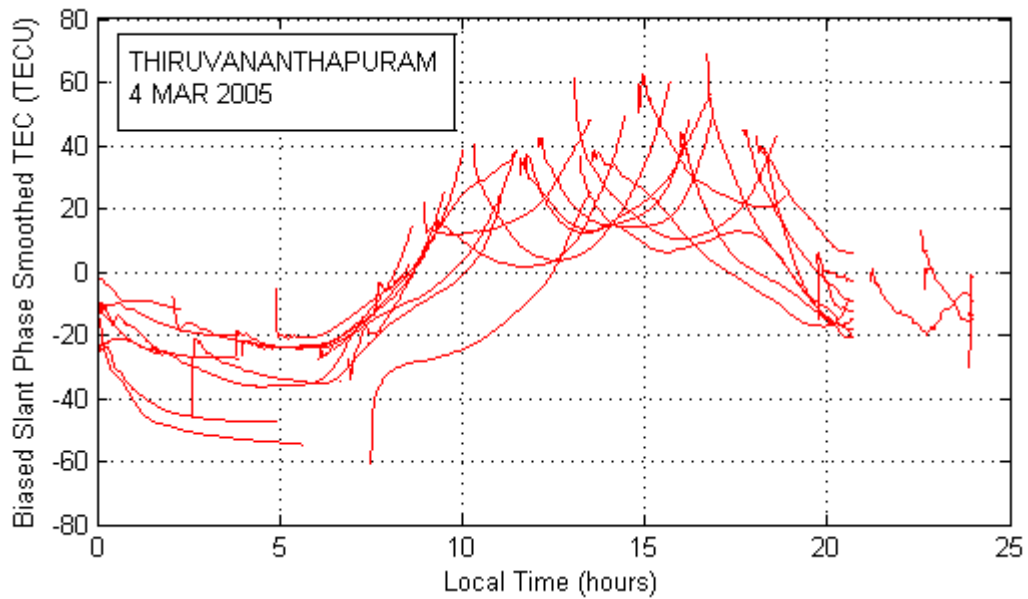


**Fig. 17** Phase smoothed slant TEC using Hatch smoothing filter (Thiruvananthapuram)

The corresponding estimated vertical TEC after removing the instrumental bias error is shown in Fig. 18.

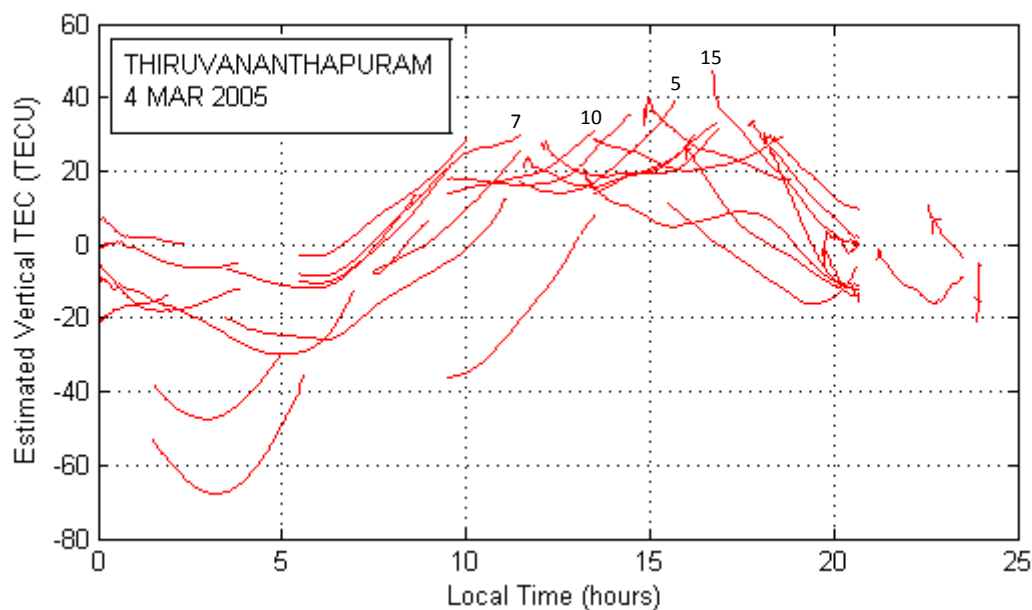


**Fig. 18** Estimated vertical TEC after correcting for instrumental biases (Thiruvananthapuram)

The estimated maximum vertical TEC of two satellites, viz. PRN 10 and PRN 5 visible during mid-day, after correcting for instrumental biases are 35.3 and 39.0 TECU. The estimated mean value of receiver bias due to various satellites using Kalman filter is -2.6 ns.

### Conclusion

The ionospheric delay (TEC) should be estimated accurately for determining position of a user precisely. In this paper, two prominent ionospheric delay smoothing algorithms are used for improving the accuracy of ionospheric delay estimation using the dual frequency GPS data. The smoothing results are validated with the Bernese GPS data processing software. Both CCCSF and HSF algorithms closely follow Bernese output, but the advantage of the Hatch filter technique is that it is simple to implement and requires less time for convergence as compared to CCCSF. The two proposed algorithms can be used for real-time ionospheric modeling keeping in view of their recursive form. For estimation of instrumental biases, the Kalman filter technique proved to be very promising and can be applied easily to many other stations. The work presented here would be useful for enhancing the performance of the present and proposed CNS systems including GAGAN.

### Acknowledgments

Thanks are due to Director, Space Applications Centre, ISRO, Ahmedabad, India for providing the data. The work presented in this paper is carried out under the project sponsored by the Department of Science and Technology, New Delhi, India, vide sanction order No. SR/S4/AS-230/03, dated 21-03-2005.

**References:**

El-Rabbany, Ahmed, “Introduction to GPS: the Global Positioning System”, Artech House, Inc., USA, 2002.

Gao, Y., Liao, X., and Liu, Z.Z., “Ionosphere Modeling Using Carrier Smoothed Ionosphere Observations from a Regional GPS Network”, *Geomatica*, Vol. 56, No. 2, pp. 97-106, 2002.

Hatch, R., “The Synergism of GPS Code and Carrier measurements”, *Proceedings of the Third International Geodetic Symposium on Satellite Doppler Positioning*, New Mexico State University, NM, USA, 8-12 February, Vol.2, pp. 1213-1231, 1982.

Hugentobler, U., Schaer, A., and Fridez, P., “Documentation of the Bernese GPS Software Version 4.2”, *Astronomical Institute, University of Berne, Switzerland*, 2001.

Misra, P., and Enge, P., “Global Positioning System Signals, Measurements, and Performance”, *Ganga Jamuna Press, MA, USA*, 2001.

Sunehra Dhiraj, Satyanarayana, K., Viswanadh, C.S., and Sarma, A.D., “Estimation of Total Electron Content and Instrumental Biases of Low Latitude Global Positioning System Stations using Kalman Filter”, *IETE Journal of Research*, Vol. 56, No. 5, September-October, pp. 235-241, 2010.

Suryanarayana Rao, K.N., “GAGAN – The Indian Satellite Based Augmentation System”, *Indian Journal of Radio & Space Physics*, Vol. 36, No. 4, pp. 293-302, August 2007.

Website 1: <http://www.insidegnss.com/node/3010>.